Engineering Failure Analysis 118 (2020) 104852

Contents lists available at ScienceDirect

Engineering Failure Analysis

journal homepage: www.elsevier.com/locate/engfailanal

Fatigue crack growth under corrosive environments of Ti-6Al-4V specimens produced by SLM

J.S. Jesus[a], L.P. Borrego[a,b,*], J.A.M. Ferreira[a], J.D. Costa[a], C. Capela[a,c]

[a] Univ Coimbra, CEMMPRE, Department of Mechanical Engineering, P-3004 516 Coimbra, Portugal
[b] Department of Mechanical Engineering, Coimbra Polytechnic - ISEC, Rua Pedro Nunes, 3030-199 Coimbra, Portugal
[c] School of Technology and Management, Polytechnic Institute of Leiria, P2411-901 Leiria, Portugal

ARTICLE INFO

Keywords:
Additive manufacturing
Corrosion-fatigue
Crack propagation
Titanium TiAl6V4 alloy

ABSTRACT

Additive manufactured parts made of Ti-6Al-4V alloy are increasingly used in medical devices and in the aeronautical industry, because of its high strength, low weight and excellent biocompatibility. Most of these components work under environmentally assisted cyclic loading, i.e. under corrosion-fatigue. Anisotropic microstructure of additive manufactured materials significantly influences the propagation of cracks, particularly under corrosion-fatigue. This paper presents the results of the failure mode and fatigue crack propagation study in titanium Ti-6Al-4V specimens produced by selective laser melting (SLM), under corrosive ambient. Three environment solutions were used: artificial saliva, Ringer's solution and 3.5%wt NaCl solution. Tests were performed using standard 6 mm thick compact specimens (CT) tested at R = 0.05 with frequencies of 1 and 10 Hz. The main objective was to study the effect of the corrosion potential on da/dN-ΔK curves and on the fatigue failure mechanisms. It was observed a very important accelerating effect on the crack initiation and fatigue crack propagation for tests under corrosion ambient, particularly for 3.5%wt NaCl solution, for which fatigue crack growth is 3.3 times higher in comparison with inert ambient tests.

1. Introduction

Titanium Ti-6Al-4V alloy is a light alloy characterized by having excellent mechanical properties combined with low specific weight, commonly used in biomedical applications and in automotive and aerospace components, as reported by Guo and Leu [1], Petrovic et al. [2] and Mur et al. [3]. This alloy has also excellent corrosion resistance, making it widely used in biomedical devices like in knee and hip joints and dental implants, which are subjected to corrosion-fatigue promoted by saliva and fluorine environment [4].

Additive manufacturing (AM) Ti-6Al-4V alloy is also a good challenge in aerospace applications because it allows to obtain complex and light components [5,6] in spite of its lower fatigue strength in comparison with Ti allows obtained by conventional processes. Leuders et al. [5] concluded that the porosity causes a reduction of the fatigue strength of additive manufactured Ti-6Al-4V.

Conventional casting Ti-6Al-4V alloy typically exhibits good corrosion and corrosion-fatigue resistance in different environments, when compared with steel and other metallic materials, due to its ability to form a thick and stable TiO_2 oxide layer, as noted by Dimah et al. [7] and Vilhena et al [8]. Dawson and Pelloux [9] studied the crack propagation in Ti-6Al-4V alloy for several

* Corresponding author at: Univ Coimbra, CEMMPRE, Department of Mechanical Engineering, P-3004 516 Coimbra, Portugal.
E-mail address: borrego@isec.pt (L.P. Borrego).

https://doi.org/10.1016/j.engfailanal.2020.104852
Received 16 February 2020; Received in revised form 25 July 2020; Accepted 16 August 2020
Available online 19 August 2020
1350-6307/

environments (distilled water and Na_2SO_4 solutions), concluding that the crack growth rates increase with decreasing frequency in distilled water, while addition of Na_2SO_4 leads to a frequency independent behaviour. In solutions containing chloride or bromide ions, a reversal in frequency dependence takes place at ΔK_{scc} (threshold stress intensity factor range for stress corrosion). Below this transition ΔK level, crack growth rates decrease with decreasing frequency due to passive film formation at the crack tip. On the contrary, Baragetti and Arcieri [10] obtained a reduction of about 20% in fatigue strength of Ti-6Al-4V in notched specimens tested in a 3.5%wt NaCl solution, at frequency of 10 Hz, in comparison with inert ambient tests.

Rabab et al [11] studied the electrochemical behaviour of Ti-6Al-4V alloy in NaCl solutions using different techniques. These authors found that a general tendency for the corrosion potential value (E_{corr}) to shift steadily towards nobler values indicated formation of a passive layer of TiO_2 and additional metal oxides. It was also found that E_{corr}. was shifted to more negative values and the passivation current density I_{corr} increase, both due to increasing NaCl concentration. In addition, the potentiodynamic cyclic anodic polarization measurements for Ti-6Al-4V alloy in NaCl solutions showed active, passive and *trans*-passive regions, with the reverse scan starting below the forward scan curve, indicating that the alloy was susceptible to pitting and crevice corrosion, such results were confirmed by using scanning electron microscopy. These authors defined the localized corrosion in Ti-6Al-4V alloy, which usually results in pitting or crevice formation, as multi-step process. It is generally accepted that the following four steps are involved in localized corrosion: (i) adsorption of reactive anions on the oxide covered titanium surface; (ii) reaction of the adsorbed anions with the titanium cations in the titanium oxide lattice or with the precipitated titanium hydroxide; (iii) thinning of the oxide by dissolution and (iv) direct attack of the exposed metal by the anions.

A few studies of corrosion behaviour for AM of Ti-6Al-4V alloy can be found in the literature. Dai et al. [12,13] reported the corrosion behaviour of the as Selective Laser Melted (SLM) Ti-6Al-4V alloy concluding that potentiodynamic and EIS (Electrochemical Impedance Spectroscopy) measurements show that the SLM-produced Ti-6Al-4V sample has worse corrosion resistance than the commercial Grade 5 alloy when submitted to 3.5 wt NaCl solution. Furthermore, no differences in the corrosion behaviour for the different microstructural planes were observed.

Jingjing et al. [14] studied the corrosion behaviours of Ti-6Al-4V samples produced by selective laser melting (SLM), wire and arc additive manufacturing (WAAM), and traditional rolling in 3.5% wt NaCl solution. These authors concluded that the order of corrosion resistance was SLM $<$ WAAM $<$ rolling, the main corrosion failure was pitting, the corrosion behaviour was dependent on the combination effects of microstructures including type, size, and morphology of constituent phases. These authors also concluded that, the inferior corrosion resistance of SLM samples can be improved significantly by exploiting an appropriate heat treatment to control the microstructure.

Regarding the AM of Ti-6Al-4V alloy fatigue behaviour under corrosion no studies related with this subject were found. For this reason, the present research pretends to introduce a contribution in order to understand the fatigue crack propagation in AM of Ti-6Al-4V alloy specimens submitted to corrosive environments, as well as, the influence of the tests frequency and the influence of each environment in the corrosion action before and during the fatigue crack growth tests.

2. Materials and testing procedure

The Material used in the current work was Titanium Ti-6Al-4V Grade 23 spherical powder, with a chemical composition, according with the manufacturer, indicated in Table 1.

Experimental tests were performed using 6 mm thickness compact tension (CT) specimens, supplied by Socem INPACT, Martingança, Portugal, with the final geometry and dimensions shown in Fig. 1, manufactured by Lasercusing®, with the build direction coincides with the loading direction. The samples were processed using a ProX DMP 320 high-performance metal additive manufacturing system, incorporating a 500 W fiber laser. After SLM manufacturing and surface milling, the specimens were subjected to a stress relieve heat treatment to reduce the residual stresses. The stress relieve treatment consisted of a slow and controlled heating up to 670 °C, followed by maintenance at 670 °C $\pm$ 15 °C for 5 h in argon medium at atmosphere pressure and finally by cooling to room temperature in air.

The faces of the specimens were polished and subjected to a chemical attack by Kroll's reagent. Afterwards, they were observed using a Leica DM4000 M LED optical microscope.

Fatigue crack growth tests were carried out in agreement with ASTM E647 standard [15], at room temperature using a 10 kN capacity Instron EletroPuls E10000 machine, under loading control and stress ratio of $R = 0.05$, with two frequencies of 1 and 10 Hz. The tests were conducted under constant loading amplitude, i.e. under increasing ΔK. The corrosive environment was realised by means of three solutions indicated in Table 2 and in air.

During the tests, the crack length was measured using a travelling microscope (45x) with an accuracy of 10 μm. Fig. 2 shows the experimental apparatus, in Fig. 2a) is detailed the specimen, the box with corrosive fluid and the system for the crack length measurement (traveling microscope), as well as the connections for measuring corrosion potential (electrodes). Fig. 2b) shows a detail of the box where were placed the corrosive fluid, the specimens and the electrodes. The lower bond was fabricated in stainless

Table 1
Chemical composition of the Titanium Ti-6Al-4V alloy [wt.%].

Al	V	O	N	C	H	Fe	Y	Ti
5.50–6.50	3.50–4.50	< 0.15	< 0.04	< 0.08	< 0.012	< 0.25	< 0.005	Bal.

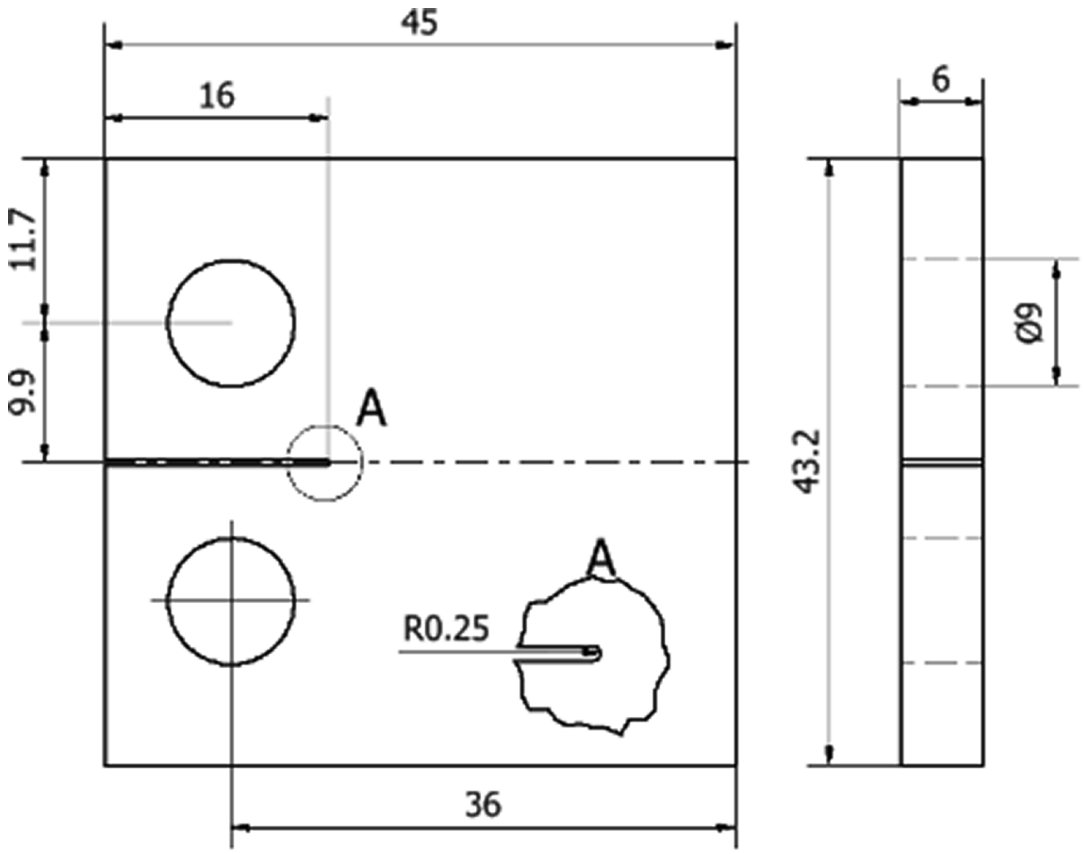

Fig. 1. Specimen geometry (dimensions in mm).

Table 2
Chemical composition of the corrosive solutions [g/l].

Corrosive solution	NaCl	K	Mg	Ca	SO_4^{2-}	KCl	$CaCl_2{\cdot}2H_2O$	KH_2PO_4	$Na_2HPO_4{\cdot}12H_2O$	KSCN	$NaHCO_3$	$C_6H_8O_7$
Saliva (pH = 6.5)	0.6	–	–	–	–	0.72	0.22	0.68	0.86	0.06	1.50	0.03
Ringeŕs (pH = 6.5)	6	–	–	–	–	0.4	0.2	–	–	–	–	–
3.5% wt NaCl (pH = 6.8)	30.2	0.39	1.3	0.42	2.7	–	–	–	–	–	–	–

steel and insulated with anti-corrosion spray, while the upper bond was not in contact with the corrosive solution.

After fatigue crack growth tests, the surfaces of fractured specimens were observed using a Philips XL30 SEM microscope.

The SP-50 Potentiostat/Galvanostat from BioLogic Science Instruments was used for electrochemical measurements with a three-electrode assembly consisting of a working electrode (WE), a reference electrode (RE), and a counter electrode (CE) as shown in the photograph presented in Fig. 2.

The corrosion resistance was evaluated by the potentiodynamic polarization method, at a scan rate of 1 mV/s. In order to determine the corrosion potential (E_{corr}) and corrosion current (I_{corr}), polarization curves, representing the current density (A/cm^2) against the potential (V vs. SCE), were obtained.

Fig. 3 shows an example of the observed microstructure, revealing a fine acicular morphology composed mainly by needles of primary α phase, heterogeneously dispersed, and a β phase distributed in the contours of the needles, quite similar to that observed by Greitmeier et al. [16] for the same material and equivalent manufacturing conditions.

3. Results and discussion

Fig. 4 presents the results obtained for the fatigue crack growth in terms of the da/dN-ΔK curves, for tests carried out at the frequency of 10 Hz, comparing the four environmental conditions studied: air, artificial saliva, Ringeŕs solution and 3.5%wt NaCl solution. Crack growth rates under constant amplitude loading were determined by the incremental polynomial method using five consecutive points. The effect of corrosion is significant in the three solutions, with an increasing of crack propagation rate of 52% under artificial saliva, 290% in Ringer's solution and more than 330% in 3.5% NaCl solution, in comparison with air environment. The results obtained confirm previous studies of Baragetti and Arcieri [10] on conventional manufactured Ti-6Al-4V alloys that observed a reduction of 20% on fatigue resistance between specimens tested in a saline solution (3.5% wt NaCl) and air.

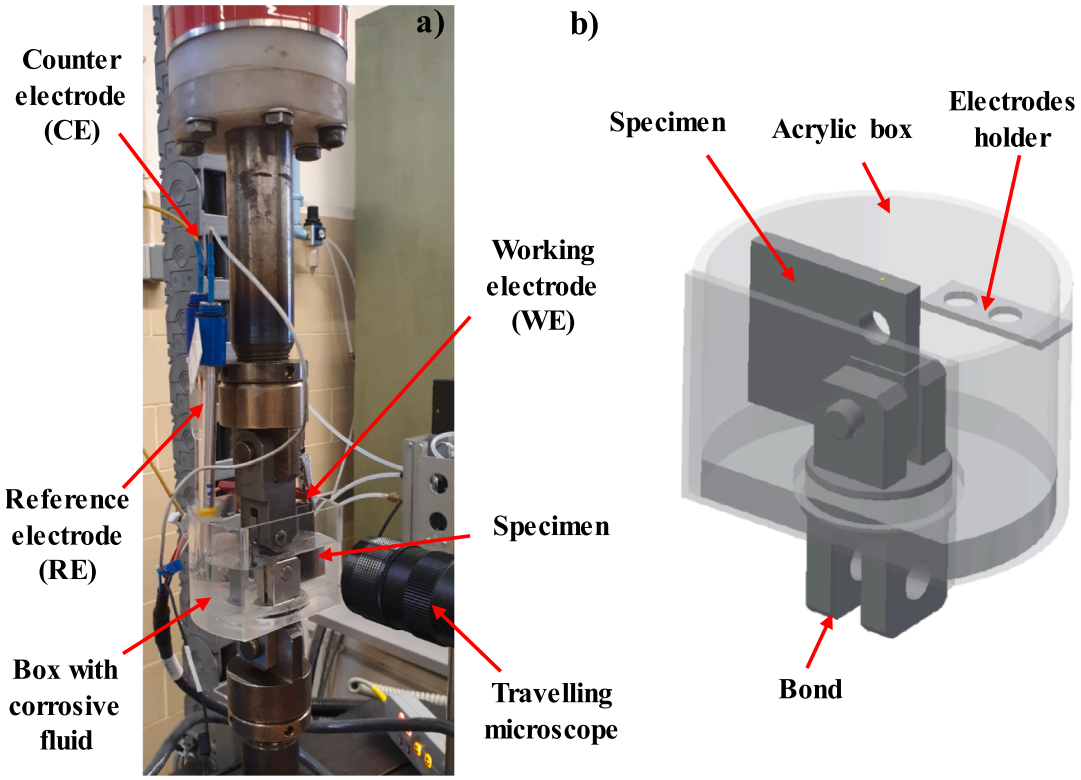

Fig. 2. Testing apparatus. a) Detail of testing apparatus and b) Detail of the corrosive box.

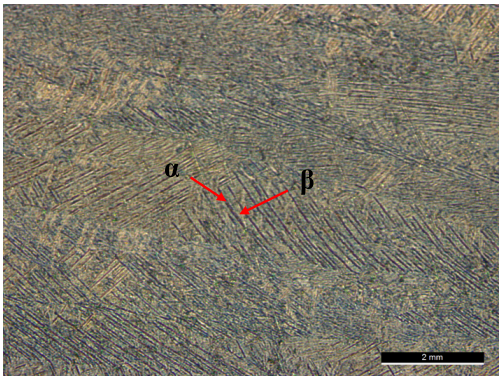

Fig. 3. Microstructure of the SLM Ti-6Al-4V alloy.

Fig. 5a), b) and c) show the effect of the loading frequency on the da/dN-ΔK curves for the different corrosive solutions: artificial saliva, Ringeŕs solution and 3.5%wt NaCl solution, respectively. In the case of artificial saliva, the reduction of frequency causes a very small effect in the Paris of crack propagation (regime II), having only a moderate damage increase for low ΔK values. Besides, Ringeŕs and 3.5%wt NaCl solutions promote an increase of crack growth rate greater than 10% in Paris regime. Table 3 resumes the Paris law parameters obtained at different load frequency and corrosive environments.

In order to justify the corrosive effect of the different solutions, its potentiodynamic polarization curves were obtained before and during the Fatigue crack growth tests. Fig. 6 shows the potentiodynamic polarization curves for the three different environments used. It can be seen that the artificial saliva environment shows a more noble behaviour than the other two environments with the corrosion potential (E_{corr}) following the direction of the decreasing potentials as follows: Artificial saliva (E_{corr} = − 314 mV) > Ringeŕs (E_{corr} = − 490 mV) > NaCl (E_{corr} = − 507 mV). The corrosion potential for the artificial saliva is the least negative. Therefore, the AM Ti-6Al-4V alloy has better corrosion resistance to artificial saliva than with to the others corrosive solutions used. This is because artificial saliva has the lowest amount of NaCl (0.6 g/l), while both Ringer's solution and 3.5% NaCl solution have higher NaCl contents, 6 g/l and 30.2 g/l, respectively.

The corrosion current density shows the following values: Artificial saliva ($i_{corr} = 5.64 \times 10^{-10}$ A/cm^2) < Ringeŕs ($i_{corr} = 3.73 \times 10^{-9}$ A/cm^2) < 3.5% NaCl ($i_{corr} = 3.16 \times 10^{-9}$ A/cm^2), while the passivation current density (i_{pass}) presented the following mean values: Artificial saliva ($i_{pass} = 7.71 \times 10^{-7}$ A/cm^2) < Ringeŕs ($i_{pass} = 8.57 \times 10^{-7}$ A/cm^2) < 3.5% NaCl ($i_{pass} = i_{pass} = 9.58 \times 10^{-7}$ A/cm^2). These values indicate that the AM Ti-6Al-4V alloy is more prone to the formation of a protective

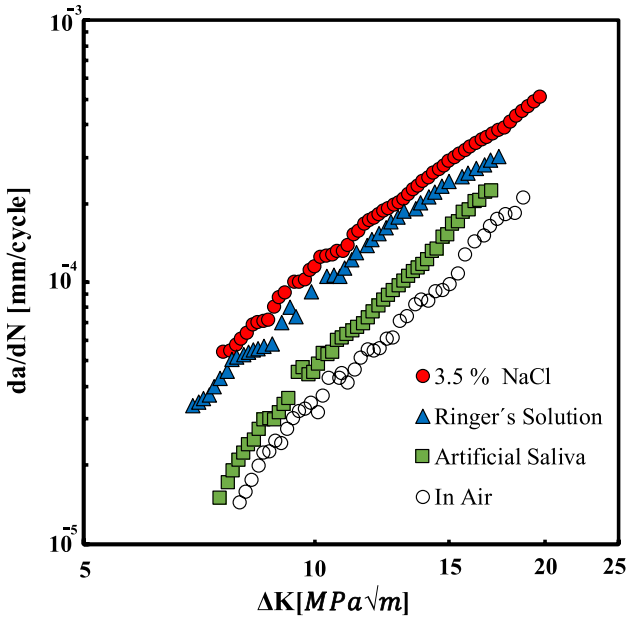

Fig. 4. Effect of corrosive solution on the da/dN-ΔK curves. Test frequency of 10 Hz.

oxide film (TiO2) in presence of artificial saliva than in the presence of artificial saliva and more difficulty to present this protection in the presence of 3.5% NaCl solution due to the amount of NaCl present in each solution. Higher percentage of NaCl increases the amount of Na^+ and Cl^- ions that attack and dissolve the protective oxide film. Therefore, it can be concluded that the most corrosion environment tested was the 3.5% NaCl solution followed by the Ringeŕs solution and the less corrosion environment was artificial saliva.

Fig. 7 shows representative examples of potentiodynamic polarization curves for three fatigue crack growth tests at 1 Hz of frequency under different environments. Potentiodynamic polarization curves were measured in the same conditions described previously for the static tests. From the analysis of Fig. 7, it can be concluded that fatigue crack growth tests started at the same corrosion potential (E_{corr}) values measured in the static tests for the three corrosive solutions, but with a strong decreasing trend during the initial period of the fatigue crack growth tests. This phenomenon is due to the solution agitation occurring during the fatigue crack growth tests, the agitation promotes a constant new source of fresh corrosive fluid accelerating the corrosive process and decreasing the corrosion potential. It means that the environment solutions become more corrosive during fatigue crack growth tests, but keeping the same order of corrosive severity: Artificial saliva $<$ Ringeŕs solution $<$ Solution with 3.5% NaCl.

As the number of cycles increase, the early crack initiation leads to a disturbance of the corrosion potential value (E_{corr}) in all environment solutions. However, these observations need a better understanding, and further tests are ongoing to confirm this relationship. Furthermore, as the fatigue cycles increase the corrosion potential (E_{corr}) decreases gradually since the crack length increases and more fractured area was available to the corrosion action. The lower corrosion action in the artificial saliva environment leads to a higher fatigue life (N_f = 430292) than for the other solutions tested: Ringeŕs solution, (N_f = 266670) and 3.5% NaCl solution (N_f = 187890). These results permit to understand the increase of the fatigue crack growth rate for the AM Ti-6Al-4V alloy under the three different corrosion environments when compared with the da/dN-ΔK curve obtained in air. The 3.5% NaCl solution showed the higher fatigue crack growth rate (the shorter fatigue life) followed by Ringeŕs solution and lastly the artificial saliva, in agreement with the corrosion severity.

Fig. 8 compares the crack path of four specimens tested under different environment conditions: a) in air, b) in artificial saliva, c) in Ringeŕs solution and d) into 3.5%wt NaCl solution. Crack path is similar for the four conditions, propagating predominantly in mode I, but with an irregular path which reveals that the crack looks for the weakest path, in most cases along the interfaces between the deposition layers. For the specimen tested in air (Fig. 8a)) it is noted that, although there is predominant crack propagation in mode I, several crack bifurcations can also be observed. However, crack growth follows always the path of the predominant crack. For the specimens tested in corrosive environments the crack path is quite similar, but the bifurcation of secondary cracks was not observed.

Finally, Fig. 9 compares SEM images of the failure surfaces for specimens tested under different environment conditions: a) in air, b) in artificial saliva and c) into 3.5%wt NaCl solution.

Failure surfaces were analyzed by scanning electron microscopy to identify the mechanisms of crack growth under corrosion assisted fatigue. Fig. 9a) shows an image taken from the fractured surface of a specimen tested in air at the Paris regime of crack propagation. The crack growth occurs transgranulary through the columnar β phase, contouring the martensitic needles of phase α, which are marked by black arrows.

Fig. 9b), depicts a SEM image taken from the fractured surface of a specimen tested at 1 Hz in the 3.5% NaCl solution. Several characteristic marks of the phenomena associated with corrosion are clearly visible. The red arrows indicate the locations affected by pitting corrosion, while the blue arrows point to the particles segregated from the pitting cavities that result from the corrosion

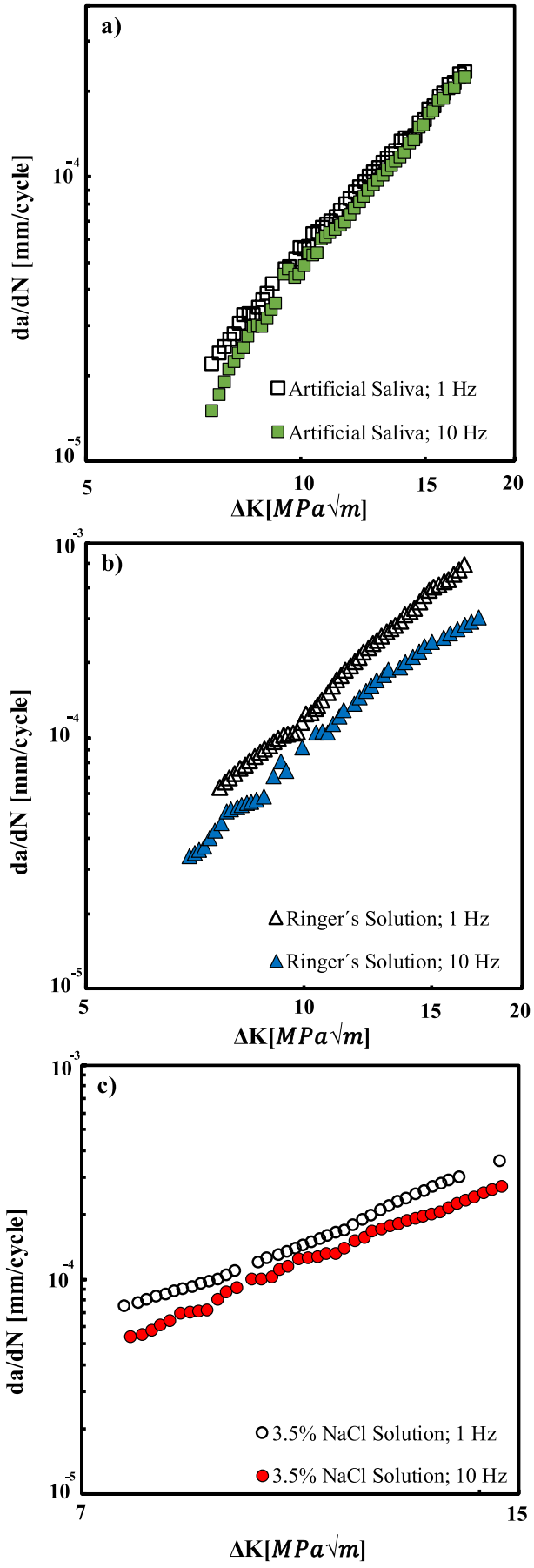

Fig. 5. Effect of the loading frequency on the da/dN-ΔK curves: a) artificial saliva; b) Ringer solution; c) 3.5%wt NaCl solution.

Table 3
Resume of Paris law parameters at different load frequency and corrosive environments. (da/dN in mm/cycle and ΔK in $MPam^{1/2}$).

Load frequency	Corrosive solution	C	m	R^2
10 Hz	Air	3.085×10^{-08}	3.011	0.991
	3.5%wt NaCl solution	4.910×10^{-07}	2.345	0.995
	Artificial Saliva	2.980×10^{-08}	3.176	0.995
	Ringeŕs solution	2.96×10^{-07}	2.471	0.992
1 Hz	3.5%wt NaCl solution	4.896×10^{-07}	2.457	0.995
	Artificial Saliva	7.516×10^{-08}	2.845	0.998
	Ringeŕs solution	2.379×10^{-07}	2.727	0.996

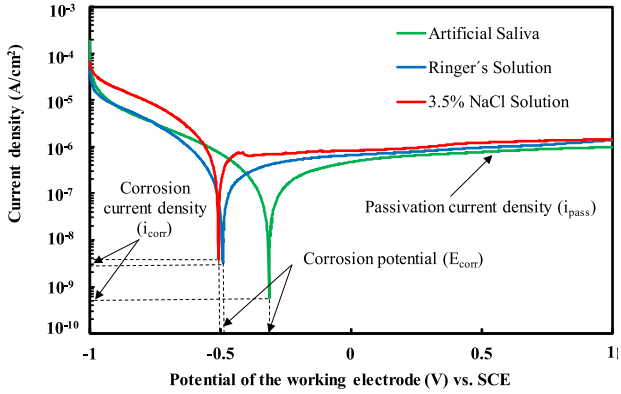

Fig. 6. Potentiodynamic polarization curves: Static test.

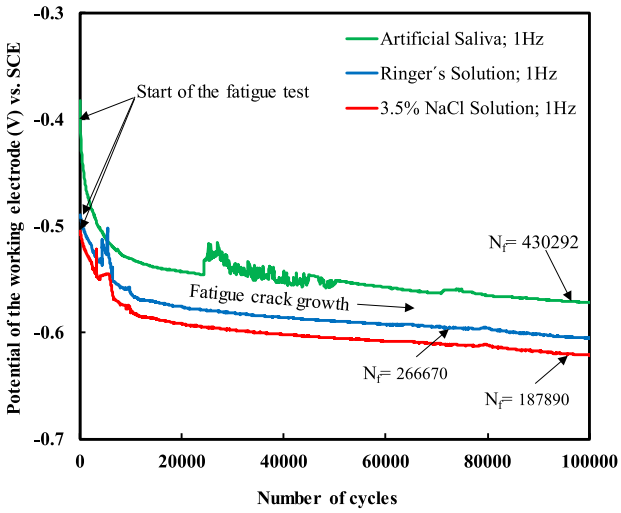

Fig. 7. Potentiodynamic polarization curves: fatigue crack growth tests at 1 Hz.

phenomenon, commonly known as crevice. Crevice corrosion marks appear near areas where pitting has occurred in the form of light-colored agglomerates containing NaCl, TiO_2 and Al_2O_3. Pitting marks occur in the form of surface depressions with a darker color. Fig. 9c) refers to a specimen tested at 1 Hz in artificial saliva. Because this solution is the least corrosive, it is noted that fewer and smaller marks are left on the surface of the crack by pitting and crevice corrosion phenomena. The blue arrow indicates what appears to be a characteristic agglomerate of the phenomenon of crevice corrosion.

These results agree with what was previously observed with the da/dN-ΔK curves, showing that NaCl solution environments cause an acceleration of fatigue crack propagation due to corrosion associated phenomena such as pitting and crevice. These phenomena have an increasing incidence with increasing NaCl content.

4. Conclusions

This study analyses the effect of corrosive solutions, namely artificial saliva, Ringeŕs solution and 3.5%wt NaCl solution, on the corrosion-fatigue behavior of TiAl6V4 specimens produced by SLM. The following conclusions can be drawn:

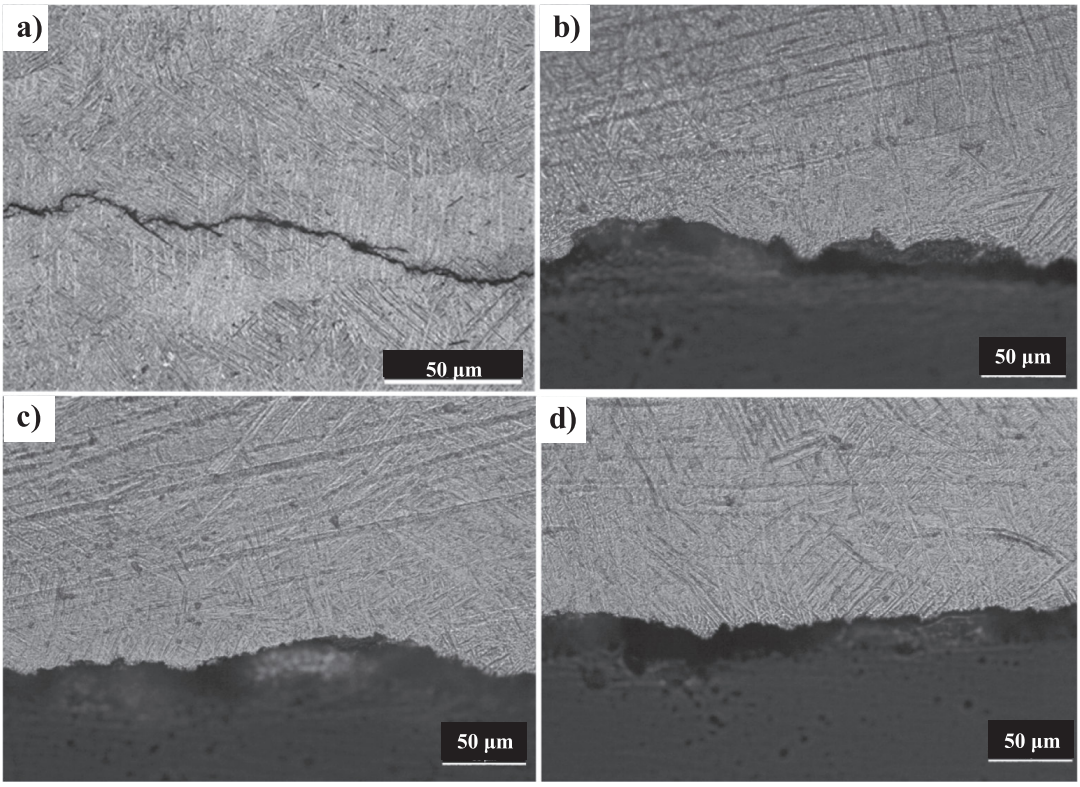

Fig. 8. Fatigue crack path: (a) In air; (b) Artificial saliva; c) Ringer solution; d) 3.5%wt NaCl solution.

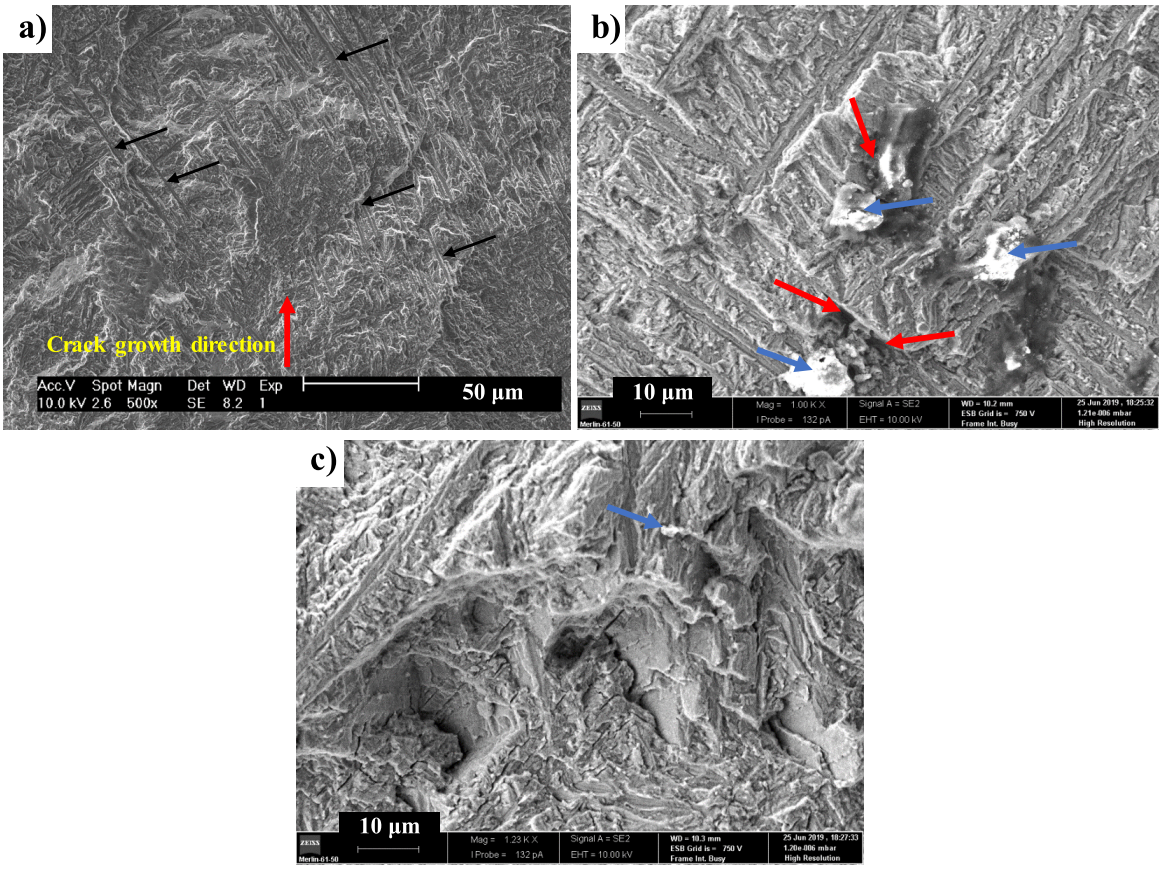

Fig. 9. SEM observations of fatigue fractured surfaces in several environments: (a) In air; (b) 3.5%wt NaCl solution; c) Artificial saliva.

- AM Titanium Ti-6Al-4V alloy exhibits a significant effect of the corrosive ambient, both on fatigue crack nucleation and on fatigue crack propagation;
- The faster corrosive effect, in comparison with the test in air, was obtained for the tests in 3.5%wt NaCl solution, for which fatigue crack growth is 3.3 times higher;
- The passivation current density, shows the following order: Artificial saliva < Ringeŕs < 3.5% NaCl, indicating that the AM Ti-6Al-4V alloy presents more facility to create a protective oxide film (TiO_2) in presence of artificial saliva and more difficulty in the presence of 3.5% NaCl solution due to the amount of NaCl present in each solution. Higher amount of NaCl in the solution causes a higher fatigue damage and crack growth rate.
- The fracture surfaces showed several characteristic marks of phenomena associated with corrosion as pitting and crevice mainly in the fatigue crack growth tests under the environment of 3.5% NaCl solution.

Declaration of Competing Interest

The authors declare that they have no known competing financial interests or personal relationships that could have appeared to influence the work reported in this paper.

Acknowledgements

The authors would like to acknowledge the sponsoring under the project no. 028789, financed by the European Regional Development Fund (FEDER), through the Portugal-2020 program (PT2020), under the Regional Operational Program of the Center (CENTRO-01-0145-FEDER-028789), and the project POCI-01-0247-FEDER-042536, financed by European Funds, through program COMPETE2020, under the Eureka smart label S0129-AddDies. Finally, acknowledge the Foundation for Science and Technology IP/MCTES through national funds (PIDDAC).

Appendix A. Supplementary data

Supplementary data to this article can be found online at https://doi.org/10.1016/j.engfailanal.2020.104852.

References

[1] N. Guo, M.C. Leu, Additive manufacturing: technology, applications and research needs, Front. Mech. Eng. 8 (2013) 215–243, https://doi.org/10.1007/s11465-013-0248-8.
[2] V. Petrovic, J.V.H. Gonzalez, O.J. Ferrando, J.D. Gordillo, J.R.B. Puchades, L.P. Grinan, Additive layered manufacturing: sectors of industrial application shown through case studies, Int. J. Prod. Res. 49 (2011) 1061–1079, https://doi.org/10.1080/00207540903479786.
[3] L.E. Murr, S.M. Gaytan, A. Ceylan, E. Martinez, J.L. Martinez, D.H. Hernandez, B.I. Machado, D.A. Ramirez, F. Medina, S. Collins, R.B. Wicker, Characterization of titanium aluminide alloy components fabricated by additive manufacturing using electron beam melting, Acta Mater. 58 (2010) 1887–1894, https://doi.org/10.1016/j.actamat.2009.11.032.
[4] R.A. Zavanelli, P.G.E. Henriques, I. Ferreira, J.M.D. de Almeida Rollo, Corrosion-fatigue life of commercially pure titanium and Ti-6Al-4V alloys in different storage environments, J. Prosthetic Dent., https://doi.org/10.1067/mpr.2000.108758.
[5] S. Leuders, M. Thöne, A. Riemer, T. Niendorf, T. Tröster, H.A. Richard, On the mechanical behaviour of titanium alloy TiAl6V4 manufactured by selective laser melting: fatigue resistance and crack growth performance, Int. J. Fatigue 48 (2013) 300–307, https://doi.org/10.1016/j.ijfatigue.2012.11.011.
[6] M. Kahlin, H. Ansell, J. Moverarem, Fatigue behaviour of additive manufactured Ti-6Al-4V, with as-built surfaces, exposed to variable amplitude loading, Int. J. Fatigue 103, (2017) 353–362, https://doi.org/10.1016/j.ijfatigue.2017.06.023.
[7] M.K. Dimah, F.D. Albeza, V.A. Borrás, A.I. Muñoz, Study of the bio tribocorrosion behavior of titanium biomedical alloys in simulated body fluids by electrochemical techniques, Wear 294–295 (2012) 409–418, https://doi.org/10.1016/j.wear.2012.04.014.
[8] L. Vilhena, G. Oppong, A. Ramalho, Tribocorrosion of different biomaterials under reciprocating sliding conditions in artificial saliva, Lubr. Sci. (2019) 1–17, https://doi.org/10.1002/ls.1478.
[9] D. Dawson, R.M. Pelloux, Corrosion fatigue crack growth of titanium alloys in aqueous environments, Metall Trans 5 (3) (1974) 723–731, https://doi.org/10.1007/BF02644669.
[10] S. Baragetti, E.V. Arcieri, Corrosion fatigue behavior of Ti-6Al-4V: Chemical and mechanical driving forces, Int. J. Fatigue 112 (2018) 301–307, https://doi.org/10.1016/j.ijfatigue.2018.02.033.
[11] Rabab M. Abou, Shahba, Waffa A. Ghannem, Azza El-Sayed El-Shenawy, Amal S.I. Ahmed, Safaa M. Tantawy, Corrosion and Inhibition of Ti-6Al-4V Alloy in NaCl Solution, Int. J. Electrochem. Sci. 6 (2011) 5499–5509.
[12] N. Dai, L.C. Zhang, J. Zhang, Q. Chen, M. Wu, Corrosion behavior of selective laser melted Ti-6Al-4 V alloy in NaCl solution, Corros. Sci. 102 (2016) 484–489, https://doi.org/10.1016/j.corsci.2015.10.041.
[13] N. Dai, L.C. Zhang, J. Zhang, X. Zhang, Q. Ni, Y. Chen, M. Wu, C. Yang, Distinction in corrosion resistance of selective laser melted Ti-6Al-4V alloy on different planes, Corros. Sci. 111 (2016) 703–710, https://doi.org/10.1016/j.corsci.2016.06.009.
[14] Jingjing Yang, Huihui Yang, Yu. Hanchen, Zemin Wang, Xiaoyan Zeng, Corrosion Behavior of Additive Manufactured Ti-6Al-4V Alloy in NaCl Solution, Metall. Mater. Trans. A 48 (7) (July 2017) 3583–3593, https://doi.org/10.1007/s11661-017-4087-9.
[15] ASTM E647 (2016) ASTM E647—standard test method for measurement of fatigue crack growth rates. ASTM B. Stand., 03(July) 1–49. www.astm.org.
[16] D. Greitemeier, D. Palm, F. Syassen, T. Melz, Fatigue performance of additive manufactured Ti-6Al-4V using electron and laser beam melting, Int. J. Fatigue 94 (2017) 211–217, https://doi.org/10.1016/j.ijfatigue.2016.05.001.